A Transgenic Mouse Line with a 58-kb Fragment Deletion in Chromosome 11E1 That Encompasses Part of the Fam20a Gene and Its Upstream Region Shows Growth Disorder

CHUNYING AN[1], YOSHI-HIRO IDE[1], MOTOKO NAGANO-FUJII[1], SOHEI KITAZAWA[2], IKUO SHOJI[1] and HAK HOTTA[1*]

[1]*Division of Microbiology, Kobe University Graduate School of Medicine, 7-5-1 Kusunoki-cho, Chuo-ku, Kobe 650-0017, Japan.*

[2]*Division of Molecular Pathology, Kobe University Graduate School of Medicine, 7-5-1 Kusunoki-cho, Chuo-ku, Kobe 650-0017, Japan.*

ABSTRACT

Growth disorder is an umbrella term for a range of abnormal growth patterns, such as unusually fast or slow growth in infants or children. The causes of growth disorder include hormonal irregularities, chronic disease, complications during pregnancy or genetic conditions. A complex trait such as body size is influenced by multiple genes as well as environmental factors, giving rise to a continuous spectrum of phenotypes. This causal complexity makes discovery of the genetic determinants of growth disorder rather difficult. We here report our discovery of a transgenic mouse line exhibiting growth disorder, which we happened to discover in the course of generating transgenic mice expressing a viral gene. Although these mice did not express any corresponding viral mRNA or protein due to a deletion in the transgene, they showed slow growth in the 5 weeks after birth and ceased growing thereafter, while maintaining a weight equivalent to that of 3-week-old normal mice. Histopathological analysis of the organs of these mice revealed that malnutrition and metabolic disorder occurred at 5 weeks after birth in the liver. Genetic analysis has revealed that the growth disorder is associated with a 58-kb fragment deletion in chromosome 11E1 that encompasses part of the Fam20a gene and part of its upstream region. The present study thus points out for the first time the possible link between Fam20a mutation and growth disorder.

INTRODUCTION

Growth disorder is an umbrella term for a range of abnormal growth patterns, such as unusually fast or slow growth in infants or children. Although hormones play a major role in growth disorder, there are numerous other etiologic factors. Chronic diseases such as heart and kidney problems, cystic fibrosis, juvenile rheumatoid arthritis, and sickle cell anemia may slow growth in some cases. Complications during pregnancy, such as some infections during pregnancy and certain genetic diseases, can also cause growth disorder. Other important factors are genetic. For example, Turner syndrome is often the culprit in

girls with arrested growth (4); this disease results when one X chromosome is present instead of two, or when one of the X chromosomes is abnormal.

In classic Mendelian traits such as eye color, the presence of a small number of discrete forms suggests that the phenotype is controlled by a very small number of genes. In contrast, a complex trait such as body size is influenced by multiple genes as well as environmental factors, giving rise to a continuous spectrum of phenotypes. This causal complexity makes discovery of the genetic determinants of growth disorder very difficult. A study on hybrid mice which investigated the possible causes for hybrid growth disorders revealed that gene imprinting has a major effect (8). The study also showed that the growth disorder most commonly affected the heterozygous sex, as expected by Haldane's rule. We here report our discovery of a transgenic (Tg) mouse line exhibiting growth disorder, which we discovered in the course of generating Tg mice expressing a viral gene. Although these mice did not express any corresponding viral mRNA or protein due to a deletion in the transgene, they showed slow growth in the 5 weeks after birth and ceased growing thereafter, while maintaining a weight equivalent to that of 3-week-old normal mice. Genetic analysis has revealed that the growth disorder is associated with a 58-kb fragment deletion in chromosome 11E1 that encompasses part of the Fam20a gene, which has recently been reported to encode an evolutionarily conserved family of secreted proteins (6).

MATERIALS AND METHODS

Plasmid construction

To ensure a high expression level in the liver, we utilized expression vector pBEP*Bgl*II (2, 3), which contains the hepatitis B virus regulatory elements. The N-terminal fragment of NS3 was obtained from digested pcDNA3.1/NS3 (H5-5 200) (1) by using *Eco*RI and *Afl*II. The fragment was subcloned into pSG5 (Stratagene). The *Bam*HI fragment obtained from pSG5/NS3 (H5-5 200) was subcloned into the *Bgl*II site of pBEP*Bgl*II vector. It was designated pBEP/NS3 (H5-5 200).

Production of Tg mice

The 1.4kb *Eco*RI-*Pst*I fragment (Fig. 1A) from pBEP/NS3 (H5-5 200) was purified by using a QIAEX II Gel Extraction Kit (QIAGEN) and microinjected into mouse embryos from the C57BL/6N strain (Clea Japan Inc.). Tg mice were identified by subjecting 100 ng of tail DNA to amplification by PCR using two sets of oligonucleotides as primers. Oligonucleotides NS3 (H5-5)-N-F (5'-CCTATCACGGCCTACTCCCAGCAGA-3') and NS3 (H5-5 200)-C-R (5'-TTGGAATGTTTGCGGAACGGCC-3') were used to amplify a 591-bp fragment from the NS3 gene. Oligonucleotides HBV-17-F (5'-CCGGGGATCTGAAACCCTAA-3') and HBV-526-R (5'-CGGTGCCGATAAGTTTCGCT-3') were used to amplify a 510-bp fragment from the promoter region. The PCR amplification protocol consisted of 35 cycles of 94°C for 5 min, 94°C for 45 seconds, 55°C for 45 seconds, and 72°C for 45 seconds, followed by a final cycle of 72°C for 7 min. Mice were cared for according to institutional guidelines, fed with ordinary feed (Funashi Farms, Funabashi, Japan) and maintained in specific pathogen-free conditions. All of the animal experiments were carried out according to the protocol approved by the Ethics Committee for Animal Experiments at Kobe University.

Analysis of transgene mRNA expression

Total RNA was extracted from the liver with an RNeasy Mini Kit (QIAGEN). A hundred ng total RNA was reverse-transcribed and amplified using SuperScript One-step RT-PCR

(Invitrogen). The following primers were used for the RT-PCR: H5-5 38-F (5'-TACTCGGTTGCATCGTCACT-3') and H5-5 335-R (5'-TCAGCATGTCTCGTGACCAA-3') for mRNA of NS3.

Analysis of Southern blotting

Genomic DNA was obtained from mouse tails by proteinase K digestion followed by phenol-chloroform-isoamylalcohol extraction and ethanol precipitation. Southern blotting was performed following the protocol provided in the DIG High Prime DNA Labeling and Detection Starter Kit II (Roche). In brief, 10 μg of genomic DNA was digested with *Bam*HI, separated by electrophoresis on a 0.8% agarose gel, and transferred to Hybond N+ nylon membranes (GE Health Care), followed by overnight hybridization at 37°C for the probe (591 bp), which was prepared by PCR using plasmid pBEP/NS3 (H5-5 200) as a template. Primers NS3 (H5-5)-N-F and NS3 (H5-5 200)-C-R were used for the probe. After stringent washing according to the manufacturer's instructions, the signal was detected by exposing the membrane to CSPD substrate for 1 hour in a dark room.

Inverse PCR analysis of the flanking sequence of the inserted transgene

Genomic DNAs extracted from the tails of Tg mice of a particular line (the lineage 230) were digested with *Bam*HI and ligated with a Ligation-Convenience Kit (Nippon Gene). After treatment with phenol:chloroform and ethanol precipitation, 100 ng of DNA was used for inverse PCR (7). Two primer sets, H5-5 38-R (5'-AGTGACGATGCAACCGAGTA-3'), H5-5 335-F (5'-TTGGTCACGAGACATGCTGA-3') and H5-5 N-R (5'-TCTGCTGGGAGTAGGCCGTGATAGG-3'), H5-5(200) C-F (5'-GGCCGTTCCGCAAACATTCCAA-3') were used for two continuous PCR analyses. Nucleotide sequences of the amplified fragments were determined by direct sequencing without subcloning using a Big Dye Deoxy Terminator cycle sequencing kit and ABI 337 DNA sequencer (Applied Biosystems).

Histopathological analysis

Tissue specimens were fixed in 4% paraformaldehyde, dehydrated in an increasing sequence of ethylalcohol solutions, and embedded in paraffin. The specimens were then sectioned at a thickness of 5 μm and stained with hematoxylin-eosin (HE) and Periodic Acid-Schiff (PAS).

RESULTS
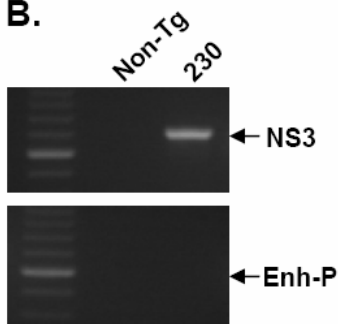
Generation of Tg mice with growth disorder

A Tg mouse line with growth disorder was generated (the lineage 230). PCR analysis revealed that these mice had a defective transgene without the enhancer-promoter region (Fig. 1B). It should be noted that, in parallel experiments, Tg mouse lines harboring the expected size of the transgene and expressing its mRNA were successfully generated (data not shown). In the lineage 230 of Tg mice, the transgene mRNA expression was not detected in the liver (Fig. 1C). These results suggested that the transgene was silenced in these mice. By mating, the defective transgene was successfully transmitted to the offspring of this Tg mouse lineage.
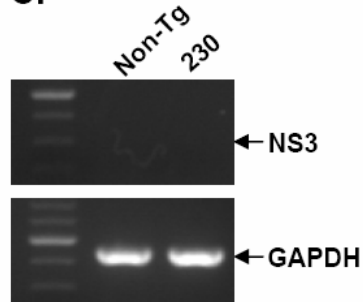
Fig. 1. Characterization of the transgene. (A) Schematic representation of the 1.4kb *Eco*RI-*Pst*I fragment used for construction of the Tg mouse. Enh-P, enhancer-promoter; A, polyadenylation signal. (B) PCR analysis of the transgene in the mouse genome. (C) RT-PCR analysis of the transgene mRNA expression. GAPDH was used as a control.

The F1 of the lineage 230 of Tg mice were hybridized together, and growth disorder progeny were found in the F2 generation. As shown in Fig. 2A, the weight of non-Tg mice (normal controls) at 5 weeks post-birth was 15.6 g (Fig. 2A, right). But the weight of a Tg mouse (littermate) at 5 weeks post-birth was only 7.9 g (Fig. 2A, left), which is similar to the weight of a 3-week-old normal mouse. However, not all littermates of the Tg mice showed the growth disorder. In the mouse with the growth disorder, no other clear abnormalities were observed. An anatomical study also showed no visible abnormality in shape and position of the organs, except for the smaller size (Fig. 2B).
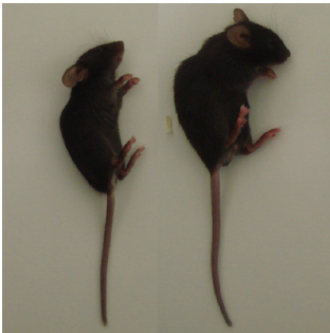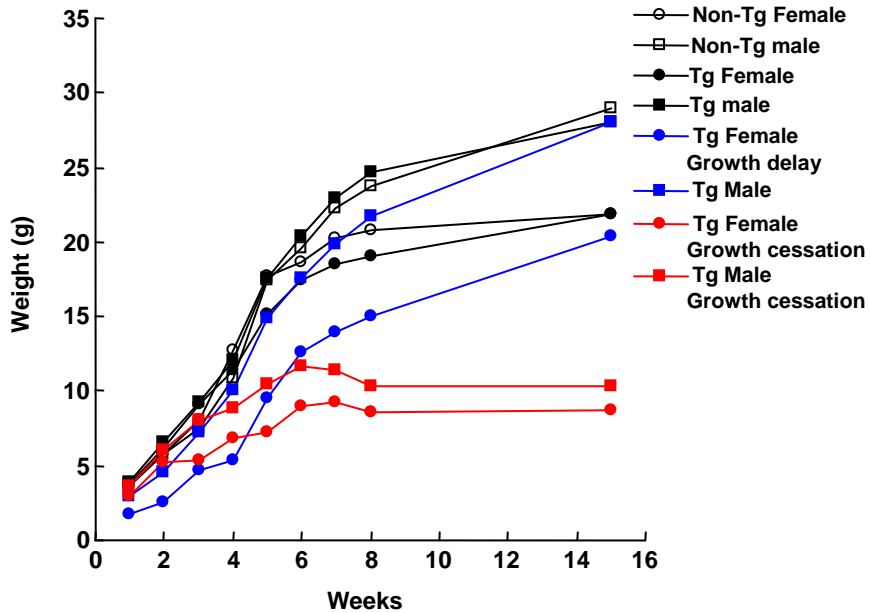
C.

Fig. 2. Phenotypes of the Tg mice. (A) 5-week-old littermates of the F1 of the lineage 230 of Tg mice with or without growth disorders. The weight of the control mouse (right) was 15.6 g, and that of the growth-cessation Tg mouse (left) was 7.9 g. (B) Gross appearance of the organs of the mice shown in (A). (C) Body weights of the progeny of the mice were measured at 1, 2, 3, 4, 5, 6, 7, 8 and 15 weeks after birth. The results for growth-cessation mice are shown as a red line, and those for the growth-delay mice are shown as a blue line.

We measured the body weight of the progeny of Tg mice at fixed time points, and produced a growth curve based on the weight of 1-15 week-old progeny (Fig. 2C). By analyzing the growth of the progeny, three growth patterns were identified: normal, growth delay and growth cessation. In the growth-cessation mice, which are represented by a red line in Fig. 2C, a growth delay was observed during the first week of life compared with normal mice. Slow growth was observed during the following 4 weeks, and then these mice stopped growing and their weight remained at the same level as the 3-week-old normal mice. In the growth-delay mice, which are represented by a blue line in Fig. 2C, a growth delay was observed during the first 8 weeks of life compared with the normal mice. These mice then gained weight gradually, and at 15 weeks post-birth, their body weight was almost normal. All of the Non-Tg mice grew normally.

Histopathological analysis of the organs of growth disorder mice

Histopathological findings of the growth disorder mice were examined by HE and PAS stainings. In the liver sections of the 5-week-old growth-cessation mice, hepatocytes were rather small, and pale cytoplasm was observed in comparison with the control mice. We speculated that this change might have been caused by the impaired accumulation of glycogen. We therefore performed PAS staining analysis. The PAS staining results of the control mice showed a rich and even distribution of glycogen (Fig. 3C). On the other hand, the liver slices of the growth-cessation mice showed uneven, faint PAS staining in the region

around the portal area (Fig. 3D), due probably to the uneven distribution of the reduced glycogen. The results for the 15-week-old growth-cessation mice were very similar to those for the 5-week-old growth-cessation mice (data not shown). These results suggested that the malnutrition or the metabolic disorder had already occurred at 5 weeks of age in the growth-cessation mice.
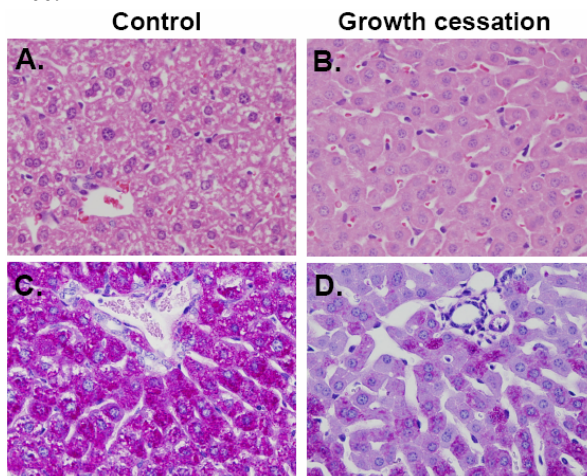

Fig. 3. Histopathological analysis of the liver of the Tg mice. (A, B) HE staining of the liver of the 5-week-old control and growth-cessation mouse, respectively. (C, D) PAS staining of the liver of the 5-week-old control and growth-cessation mouse, respectively.

Moreover, as shown in Fig. 4A and 4B, the mucosa of the gastro-intestinal (GI) tract, presented a wide range of defective-growth patterns in the 15-week-old growth-cessation mice compared with the control group. It should be noted that such changes in the mucosa of the GI tract were not observed in the 5-week-old growth-cessation mice (data not shown).

The skin of the 15-week-old growth-cessation mice lacked the fat layer between the dermis and muscular layer. The growth of the muscular layer was poor, and the adipocytes beneath it were relatively small and show immature features (Fig. 4C, D.). Such changes were not observed in the 5-week-old growth-cessation mice (data not shown).

No clear histopathological changes were observed in the other organs of either the 5- or 15-week-old growth-cessation mice, except for the smaller size.
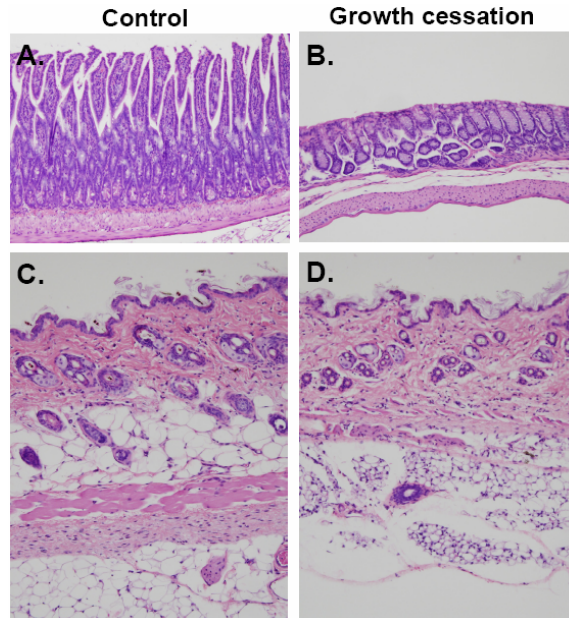
Fig. 4. Histopathological analysis of the intestine and skin of the Tg mice. (A, B) HE stainings of the intestine of the 15-week-old control and growth-cessation mice, respectively. (C, D) HE stainings of the skin of the 15-week-old control and growth-cessation mice, respectively.

Taken together, the results suggested that malnutrition and metabolic disorder occurred at 5 weeks of age in the liver of growth-cessation mice. The mucosa of the GI tract presented a wide range of defective-growth patterns in the 15-week-old growth-cessation mice compared with the controls, which may have further deteriorated the malnutrition and the metabolic disorder.

Identification of a 58-kb fragment deletion in chromosome 11E1 that encompasses part of the Fam20a gene and its upstream region of the Tg mice with growth disorder

Next, we investigated the cause of the growth disorder in the Tg mouse lineage. In light of the fact that the growth disorder appeared in transgenic mice without the expression of the transgene, we hypothesized that it was probably caused by genetic mutation through the introduction of the transgene. First, we attempted to identify the insert position of the transgene. Southern blot analysis of the *Bam*HI-digested chromosomal DNA revealed that the transgene has been introduced into only one site in the mouse's genome (Fig. 5A). Next, the transgene-containing *Bam*HI fragment, which is about 5 kb in length, was self-ligated and then amplified by using inverse PCR. The 4.5-kb fragment, which is thought to be the complete length, was amplified by inverse PCR. In addition, a 1.5-kb fragment, a 2.0-kb fragment and a 1.0-kb fragment were also amplified (Fig. 5B). Eight samples that included fragments of each of these lengths were chosen for sequence analysis. The results of the sequence analysis showed that all of the fragments possessed the same flanking sequence to the transgene. This result was consistent with the results of the Southern blot analysis. Other primers that were located in the sequence flanking the transgene were designed for cloning the transgene and the flanking sequence, and sequence analysis was conducted (Fig. 5C). We searched for the sequence in the NCBI data base, and found that the transgene has been inserted into chromosome 11E1. This transgene insertion resulted in the deletion of a 58-kb genome fragment encompassing part of the Fam20a gene, including exon 1, and its upstream region (Fig. 5D).
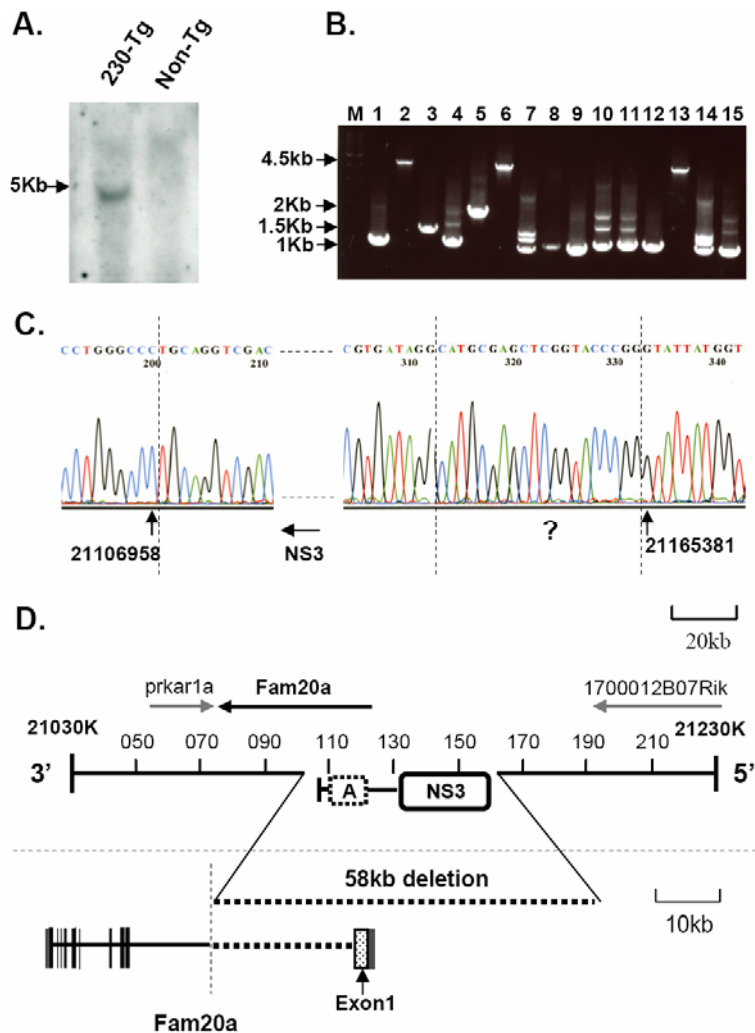
Fig. 5. Identification of a 58-kb fragment deletion in chromosome 11E1 that encompasses part of the Fam20a gene and its upstream region. (A) Genomic DNA was obtained from mouse tails by proteinase K digestion followed by phenol-chloroform-isoamylalcohol extraction and ethanol precipitation. The DNA was digested with *Bam*HI and subjected to Southern blot analysis. (B) The NS3-*Bam*HI fragment was amplified by using inverse PCR. A 4.5-kb fragment (lanes 2, 6 and 13), which is thought to be the complete length, a 1.5-kb fragment (lane 3), a 2.0-kb fragment (lane 5) and a 1.0-kb fragment (lanes 1, 4, 7, 8, 9, 10, 11, 12, 14 and 15) were amplified by using inverse PCR. (C) The transgene (NS3)-flanking sequence in the chromosome 11E1 that encompasses part of the Fam20a gene and its upstream region. (D) Schematic representation of the Fam20a gene with the deletion and inserted transgene. A 58-kb fragment deletion, which encompasses part of the Fam20a gene and its upstream region, is indicated by a dotted line.

From the above results, we speculated that the normal Tg mice were heterozygous with the 58-kb fragment deletion in chromosome 11E1 that encompasses part of the Fam20a gene

(58kb$^{-/+}$), while the growth-cessation and growth-delay Tg mice were homozygous progeny with the 58-kb fragment deletion (58kb$^{-/-}$).

In order to verify the correlation between the 58-kb fragment deletion and the growth disorder (growth cessation and growth delay) in this Tg mouse lineage, we performed the following intercross-breeding experiment. The genotype of 12 live-born progeny derived from this mating was analyzed by using PCR (Fig. 6A). A family tree was made (Fig. 6B), and the number of each genotype in each generation, and the number and ratio of growth-cessation progeny are summarized in Table I. Eleven (26%) of 43 heterozygous mice and 7 (70%) of 10 homozygous mice showed the growth-cessation phenotype. These results suggest that the Fam20a gene defect plays a role in the growth disorder of the Tg mice. The results also suggest that, in addition to the Fam20a gene defect, another factor(s), including an environmental one(s), is involved in triggering the growth disorder.
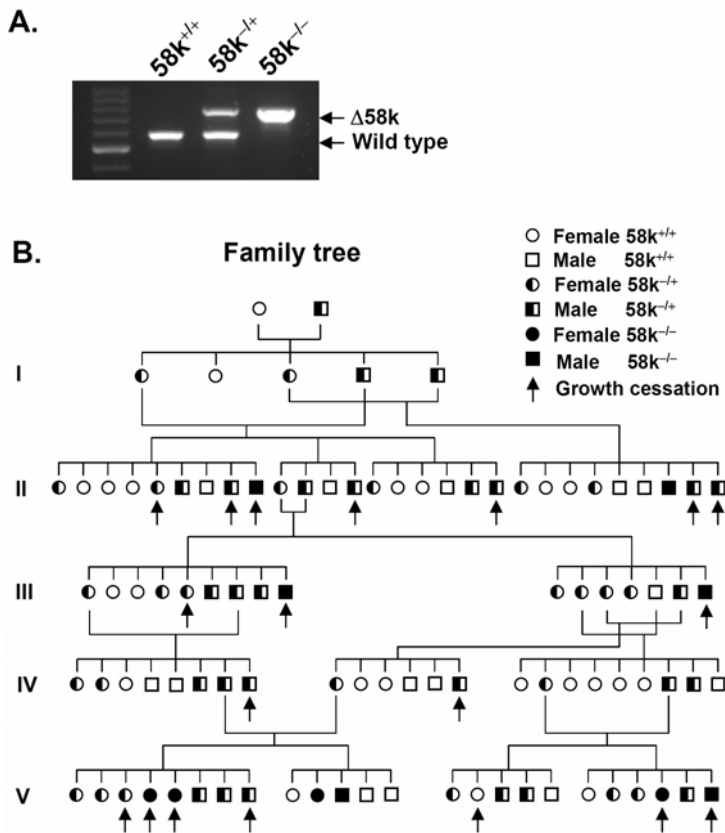

Fig. 6. Correlation between growth disorder and the 58-kb fragment deletion of chromosome 11E1 that encompasses part of the Fam20a gene and its upstream region. (A) The genotypes of 12 live-born progeny derived from intercross-breeding were analyzed by PCR. Homozygous offspring (58k$^{-/-}$) have the Δ58k band only. Wild-type offspring (58k$^{+/+}$) have the wild-type band only. Heterozygous offspring (58k$^{-/+}$) have both the Δ58k band and the wild-type band. (B) The family tree of intercross offspring of heterozygous mice of the lineage 230.

Table I. Prevalence of mice with growth disorders in the total progeny.

Generation	No. of mice with growth disorder / No. of total								
	58k+/+			58k−/+			58k−/−		
	Female	Male	Total	Female	Male	Total	Female	Male	Total
II	0 / 7	0 / 5	0 / 12	1 / 6	5 / 8	6 / 14	0 / 0	1 / 2	1 / 2
III	0 / 2	0 / 1	0 / 3	1 / 7	0 / 4	1 / 11	0 / 0	2 / 2	2 / 2
IV	0 / 3	0 / 4	0 / 7	0 / 3	2 / 4	2 / 7	0 / 0	0 / 0	0 / 0
V	1 / 3	0 / 4	1 / 7	1 / 6	1 / 5	2 / 11	3 / 4	1 / 2	4 / 6
Total	1 / 15	0 / 14	1 / 29 (3.4%)[*]	3 / 22	8 / 21	11 / 43 (26%)[*]	3 / 4	4 / 6	7 / 10 (70%)[*]

[*]Ratio of growth-cessation progeny of each genotype in total progeny of each genotype.

DISCUSSION

We accidently found a Tg mouse line exhibiting growth disorder (Fig. 2) in the course of generating Tg mice for a viral gene. The promoter of the transgene has been lost and no transgene mRNA detected in the Tg mice (Fig. 1). Therefore, the growth disorder of mice of this lineage should have nothing to do with the transgene. On the other hand, the Tg mice have undergone deletion of a 58-kb fragment, which encompasses exon 1 of the Fam20a gene (Fig. 5). The mice show impaired accumulation of glycogen in the hepatocytes at 5 weeks after birth (Fig. 3), which is thought to be a primary cause of he growth disorder.

The results of intercross-breeding analysis indicated that 70% of the homozygous offspring ($58k^{-/-}$) and 26% of heterozygous offspring ($58k^{-/+}$) showed growth cessation whereas only a single wild-type offspring (3.4%) showed growth cessation (Fig. 6; Table I). The high ratio of growth cessation in homozygous and heterozygous offspring indicate that the 58-kb fragment deletion is closely associated with the growth disorder of the Tg mice. Heterozygous ($58k^{-/+}$) mice were intercrossed to analyze the segregation of the 58-kb deletion in the Tg mice of this lineage. Of 82 offspring obtained, 10 (12.2%) were homozygous ($58k^{-/-}$), 43 (52.2%) were heterozygous ($58k^{-/+}$) and 29 (35.4%) were wild-type ($58k^{+/+}$). According to the rule of segregation, the ratio of homozygous offspring ($58k^{-/-}$) in the total should be 25%. However, the actual ratio of the homozygous offspring ($58k^{-/-}$) was only 12% (10/82). Also, the average number of live-born offspring of this lineage was 6.8, which is significantly less than that of the parental C57BL/6N line (9.0). It is likely, therefore, that homozygous offspring ($58k^{-/-}$) have some disadvantage during the early embryo growth period, including embryonic lethality. Moreover, some, but not all, homozygous ($58k^{-/-}$) and heterozygous ($58k^{-/+}$) mice showed growth delay rather than complete growth cessation (Fig. 2). These results imply the possibility that the growth disorder of this Tg mice lineage is not determined by a single factor but determined by multiple factors.

Few studies have been performed on the Fam20a protein, and its function is poorly understood. Fam20a is a member of a related protein family with 2 other members in mammals: Fam20b and Fam20c (6). Nalbant et al. (6) recently reported that Fam20a, a secreted glycoprotein, induced myeloid differentiation in the mouse EML hematopoietic stem cell line. Further studies are needed to measure the expression levels of Fam20a, and determine its role in the growth of mice.

The PAS staining of mouse liver sections showed that metabolic disorder and malnutrition occurred in the liver at 5 weeks after birth or even earlier. According to the Nalbant et al. (6), Fam20a displayed a restricted expression pattern, with high levels in the human lung and liver. The high expression of Fam20a in the liver suggests that Fam20a has something to do with development and/or functions of hepatocytes, in addition to the bone marrow differentiation (6).

ACKNOWLEDGEMENTS

REFERENCES

1. **Deng L, Nagano-Fujii M, Tanaka M, Nomura-Takigawa Y, Ikeda M, Kato N, Sada K, Hotta H.** 2006. NS3 protein of Hepatitis C virus associates with the tumour suppressor p53 and inhibits its function in an NS3 sequence-dependent manner. J Gen Virol. **87:**1703-13.
2. **Koike K, Moriya K, Yotsuyanagi H, Iino S, Kurokawa K.** 1994. Induction of cell cycle progression by hepatitis B virus HBx gene expression in quiescent mouse fibroblasts. J Clin Invest. **94:** 44-9.
3. **Koike K, Moriya K, Ishibashi K, Matsuura Y, Suzuki T, Saito I, Iino S, Kurokawa K, Miyamura T.** 1995. Expression of hepatitis C virus envelope proteins in transgenic mice. J Gen Virol. **76:** 3031-8.
4. **Lippe B.** 1991. Turner syndrome. Endocrinol Metab Clin North Am. **20:**121-52.
5. **McKusick VA, Cross HE.** 1966. Ataxia-telangiectasia and Swiss-type agammaglobulinemia. Two genetic disorders of the immune mechanism in related Amish sibships. JAMA. **195:** 739-45.
6. **Nalbant D, Youn H, Nalbant SI, Sharma S, Cobos E, Beale EG, Du Y, Williams SC.** 2005. FAM20: an evolutionarily conserved family of secreted proteins expressed in hematopoietic cells. BMC Genomics. **27:** 6(1):11.
7. **von Melchner H, Reddy S, Ruley HE.** 1990. Isolation of cellular promoters by using a retrovirus promoter trap. Proc Natl Acad Sci U S A. **87:** 3733-7.
8. **Vrana PB, Fossella JA, Matteson P, del Rio T, O'Neill MJ, Tilghman SM.** 2000. Genetic and epigenetic incompatibilies underlie hybrid dysgenesis in Peromyscus. Nature Genetics **25:** 120–124.